iScience

CellPress
OPEN ACCESS

Article

Spinal TAOK2 contributes to neuropathic pain via cGAS-STING activation in rats

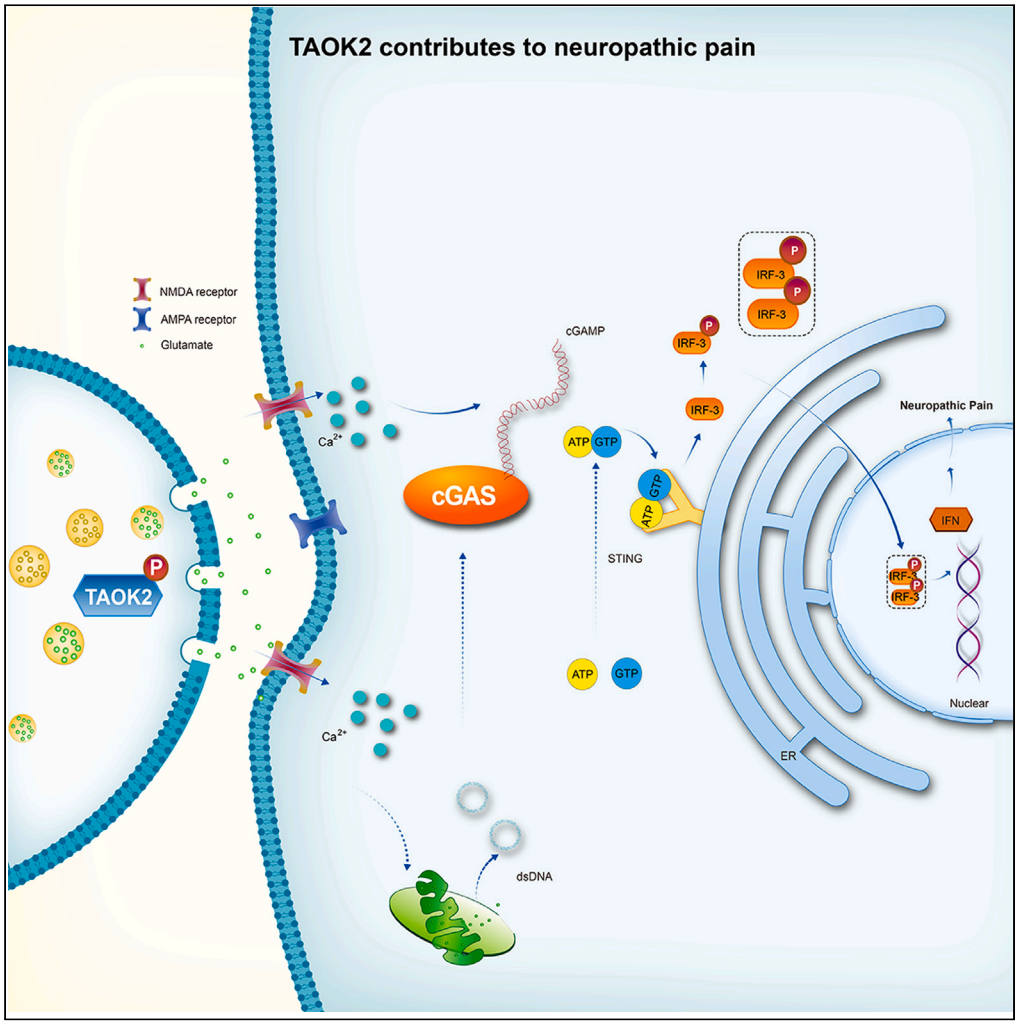

Hui Zhang, Ang Li, Yu-Fan Liu, ..., Jia-Piao Lin, Yan Yang, Yong-Xing Yao

yang_yan@zju.edu.cn (Y.Y.)
yaoyongxing@zju.edu.cn (Y.-X.Y.)

Highlights

TAOK2 is expressed in afferent nerve endings in the spinal dorsal horn

CCI-induced behavioral hyperalgesia and activation of TAOK2 and cGAS-STING signaling

Silencing TAOK2 suppressed CCI-induced upregulation of cGAS-STING

TAOK2 activation induced hyperalgesia and activated cGAS-STING in naive rats

Zhang et al., iScience 26, 107792
October 20, 2023
https://doi.org/10.1016/j.isci.2023.107792

iScience

CellPress
OPEN ACCESS

Article

Spinal TAOK2 contributes to neuropathic pain via cGAS-STING activation in rats

Hui Zhang,[1,5] Ang Li,[1,2,5] Yu-Fan Liu,[1,5] Zhong-Ming Sun,[1] Bing-Xin Jin,[1] Jia-Piao Lin,[1] Yan Yang,[3,4,*] and Yong-Xing Yao[1,6,*]

SUMMARY

Thousand and one amino acid kinase 2 (TAOK2) is a member of the mammalian sterile 20 kinase family and is implicated in neurodevelopmental disorders; however, its role in neuropathic pain remains unknown. Here, we found that TAOK2 was enriched and activated after chronic constriction injury (CCI) in the rat spinal dorsal horn. Meanwhile, cyclic guanosine monophosphate-adenosine monophosphate synthase (cGAS)-stimulator of interferon genes (STING) signaling was also activated with hyperalgesia. Silencing TAOK2 reversed hyperalgesia and suppressed the activation of cGAS-STING signaling induced by CCI, while pharmacological activation of TAOK2 induced pain hypersensitivity and upregulation of cGAS-STING signaling in naive rats. Furthermore, pharmacological inhibition or gene silencing of cGAS-STING signaling attenuated CCI-induced hyperalgesia. Taken together, these data demonstrate that the activation of spinal TAOK2 contributes to CCI-induced hyperalgesia via cGAS-STING signaling activation, providing new molecular targets for the treatment of neuropathic pain.

INTRODUCTION

Neuropathic pain is defined as a disorder caused by injury or disease of the somatosensory nervous system and is commonly characterized by spontaneous pain, hyperalgesia, or allodynia.[1,2] Accounting for 15%–25% of chronic pain, neuropathic pain significantly affects the quality of life and imposes a heavy burden on public health.[3,4] Currently, the primary modality for treating neuropathic pain is the prescription of drugs, including non-steroidal analgesics, tricyclic antidepressants, and opioids. Although new treatment methods, such as radiofrequency therapy, electrical stimulation, or surgical musculofascial release, have emerged, they are far from satisfactory and sometimes exhibit side effects.[5,6] Therefore, it is urgent to develop new therapeutic targets and strategies for clinical practice.

Although it has been considered that central and peripheral sensitization is the essential mechanism underlying the development of neuropathic pain, its pathogenesis still remains elusive.[7,8] Accumulating evidence demonstrates that the activation of protein kinase in the central nervous system plays an indispensable role in the central sensitization and maintenance of neuropathic pain[9–11]; however, the cellular and molecular mechanisms of protein kinase activation that contribute to the plasticity of neuronal cells and synaptic structural remodeling remain to be further investigated.

The gene encoding thousand and one amino acid kinase 2 (TAOK2) is located at the locus 16p11.2. TAOK2 is a serine/threonine protein kinase belonging to the mammalian sterile 20 kinase family.[12] Studies have revealed that TAOK2 is involved in stress-sensitive kinase cascades, mediates p38 activation, and is functionally implicated in cell division, cytoskeleton formation, apoptosis, and DNA damage.[13–15] In mammals, TAOK2 is found to be expressed in cerebral cortex neurons and involved in the development of neurological diseases. For example, TAOK2 may contribute to the development of autism by disturbing the formation of neuronal dendrites and the maturation of synaptic structures in the developing brain.[16–18] In addition, TAOK2 is considered to participate in accelerating the occurrence of Alzheimer's disease by promoting microtubule-associated protein phosphorylation, suggesting that TAOK2 plays important roles in the process of neurodegenerative disorders.[19,20] A recent study in *Drosophila* found that TAOK2 mediates the responsiveness of C4da neurons to mechanical stimuli, indicating a potential perception function to noxious stimuli.[21] However, the expression profile of TAOK2 in the mammalian spinal cord and its potential role in pain modulation have not been investigated.

Recent studies have revealed that peripheral nerve injury results in cellular DNA damage in the spinal cord, which leads to increased DNA fragmentation in the cytoplasm, and thus, promotes the initiation and development of neuropathic pain.[22–24] However, the biological mechanisms of DNA damage, which is involved in the development of neuropathic pain, remain largely unknown.

[1]Department of Anesthesia, First Affiliated Hospital, Zhejiang University School of Medicine, Hangzhou, Zhejiang 310003, China
[2]Department of Anesthesia, People's Hospital of Guizhou Province, Guiyang, Guizhou 550025, China
[3]Department of Neurobiology, Sir Run Run Shaw Hospital, Zhejiang University School of Medicine, Hangzhou, Zhejiang 310020, China
[4]Centre for Neuroscience, Zhejiang University School of Medicine, Hangzhou, Zhejiang 310058, China
[5]These authors contributed equally
[6]Lead contact
*Correspondence: yang_yan@zju.edu.cn (Y.Y.), yaoyongxing@zju.edu.cn (Y.-X.Y.)
https://doi.org/10.1016/j.isci.2023.107792

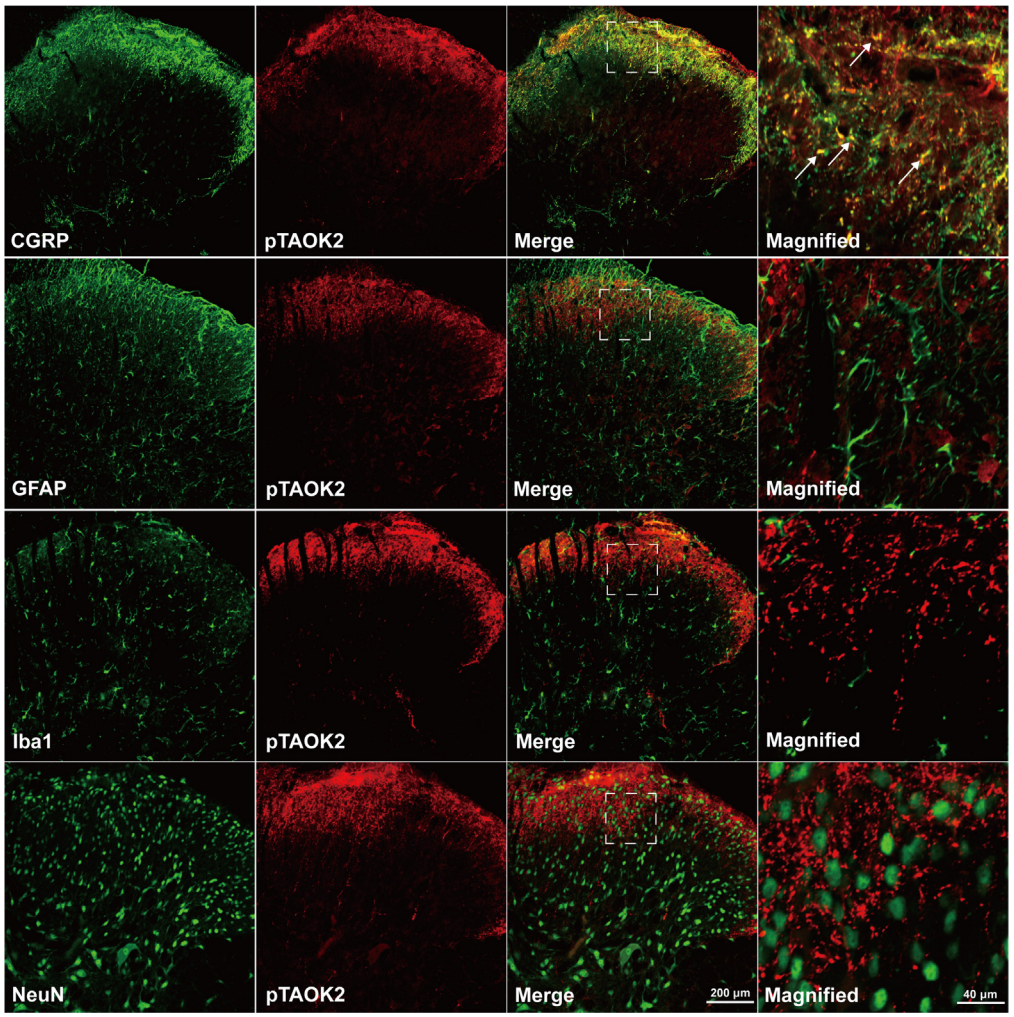

Figure 1. The expression profile of TAOK2 in the spinal dorsal horn

Double immunofluorescence staining shows colocalization of pTAOK2 with CGRP, but not with NeuN, GFAP, or Iba1. CGRP, calcitonin gene-related peptide; NeuN, neuron-specific nuclear protein; GFAP, glial fibrillary acidic protein; Iba1, ionized calcium-binding adaptor molecule-1. White arrows indicate colocalization.

Located in the cytoplasm, cyclic guanosine monophosphate-adenosine monophosphate synthase (cGAS) detects the DNA fragments of exogenous microorganisms or endogenous fragments produced by cell metabolism. The activated cGAS synthesizes the DNA sensor cyclic-GMP-AMP and subsequently stimulates the production of interferon.[25,26] On the other hand, stimulator of interferon genes (STING), upon binding to the intact endoplasmic reticulum, promotes the formation of autophagosome or cytokine (such as interferon) release, thus maintaining the homeostasis of the intracellular environment.[27,28] Therefore, cGAS-STING is believed to be an important component of the natural immune system. A recent study revealed that STING modulates physiological pain in the murine and primate spinal cord, and STING activity is negatively correlated with pain perception.[29] However, there are controversies on the role of STING in pain perception. Other reports have found that STING is positively correlated with pain via regulating the inflammatory factor interleukin-6 or suppressing microglial polarization.[30,31] Thus, the role of cGAS-STING signaling in the dorsal spinal cord in pain modulation requires further exploration.

In the present study, we explored the role of TAOK2 and the molecular mechanisms underlying its mediation of neuropathic pain. Our findings revealed for the first time that spinal TAOK2 is expressed in afferent nerve endings and contributes to neuropathic pain via activation of cGAS-STING signaling, suggesting a crucial role for TAOK2 in the development of neuropathic pain and providing new molecular targets for drug development and clinical treatment of neuropathic pain.

RESULTS

Colocalization of TAOK2 with calcitonin gene-related peptide in the spinal dorsal horn

To explore the role of spinal TAOK2 in pain modulation, we first investigated the expression of TAOK2 in the spinal cord. Double immunofluorescence staining showed that pTAOK2 was intensively expressed in the superficial layer of the spinal dorsal horn, where primary

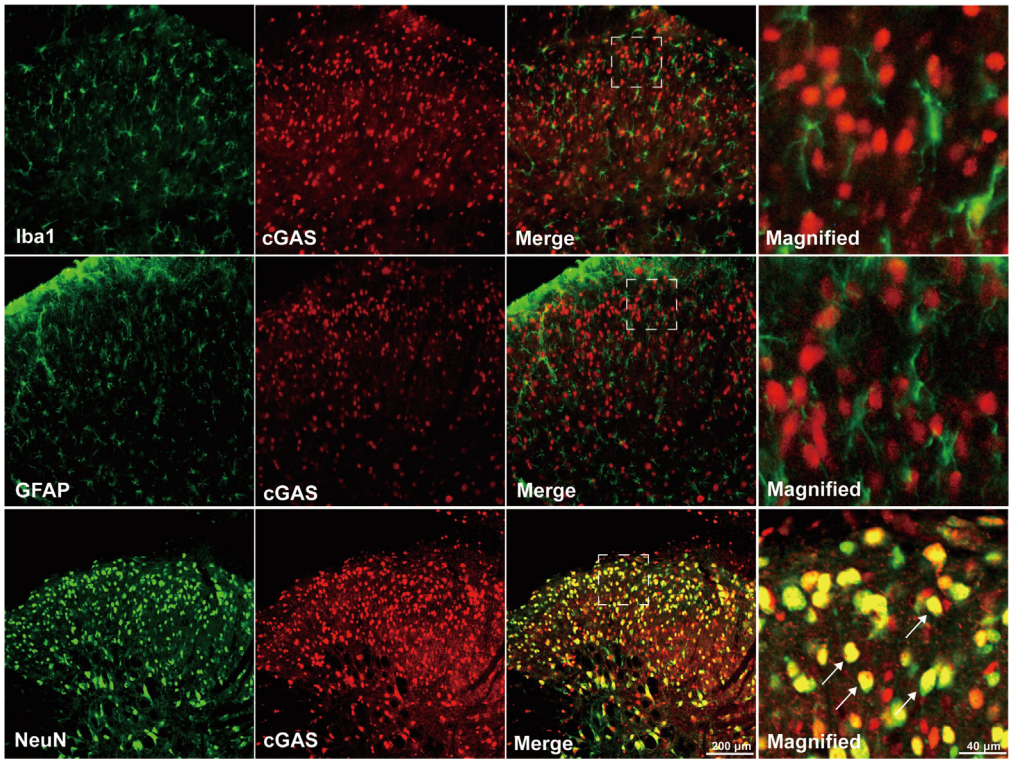

Figure 2. Colocalization of cGAS with NeuN in the spinal dorsal horn

Double immunofluorescence staining showed that cGAS colocalized with NeuN but not GFAP or Iba1. NeuN, neuron-specific nuclear protein; GFAP, glial fibrillary acidic protein; Iba1, ionized calcium-binding adaptor molecule-1. White arrows indicate colocalization.

nociceptive afferents (C/Aδ) terminate and colocalize with the afferent nerve-ending marker calcitonin gene-related peptide, but not with the neuronal marker NeuN, astrocyte marker GFAP, and microglial marker Iba1, suggesting that spinal TAOK2 was predominantly expressed on C-fibers afferent nerve endings on the superficial dorsal horn (Figure 1).

Colocalization of cGAS with NeuN in the spinal dorsal horn

To detect the expression profile of cGAS-STING in the spinal cord, double immunofluorescence staining was used. The results showed that cGAS was colocalized with NeuN and not with GFAP or Iba1, indicating that cGAS was primarily expressed in neurons in the spinal dorsal horn (Figure 2).

Colocalization of STING with NeuN, Iba1, and cGAS in the spinal dorsal horn

Double immunofluorescence staining showed that STING was colocalized with NeuN and Iba1 but not with GFAP, demonstrating that STING was not only expressed in neurons but also in microglia. Additionally, STING and cGAS colocalized well in the spinal dorsal horn (Figure 3).

CCI-induced behavioral hyperalgesia and activation of TAOK2 and cGAS-STING signaling

We conducted behavioral tests before and on day 7 after chronic constriction injury (CCI) to test the establishment of neuropathic pain. The results showed no significant differences in the baseline mechanical withdrawal threshold (MWT) and acetone test score (ATS) among the three groups. Compared to those in the sham group, the MWT significantly decreased, and ATS significantly increased in the CCI group on day 7 after CCI (Figures 4A and 4B; ***$p < 0.001$, vs. Sham, one-way ANOVA, $n = 7$), indicating that the neuropathic pain model was successfully established. Western blotting results showed that the expression of TAOK2 in the spinal dorsal horn was not significantly different 7 days after CCI (Figure 4C). However, the expression levels of phosphorylated TAOK2, cGAS, and STING in the ipsilateral spinal dorsal horn increased significantly in the CCI group (Figures 4D–4F; **$p < 0.01$, ***$p < 0.001$, vs. Sham, one-way ANOVA, $n = 4$). These results suggest that the TAOK2 and cGAS-STING signaling pathways are activated in the spinal dorsal horn during neuropathic pain.

Silencing TAOK2 reversed hyperalgesia and suppressed cGAS-STING upregulation induced by CCI

To further investigate the role of TAOK2 in neuropathic pain, siRNA was intrathecally used to knock down TAOK2 expression on days 7 and 8 after CCI (Figure 5A). Pilot experiments revealed that intrathecal application of TAOK2-siRNA (10 μg) for 2 consecutive days reduced TAOK2

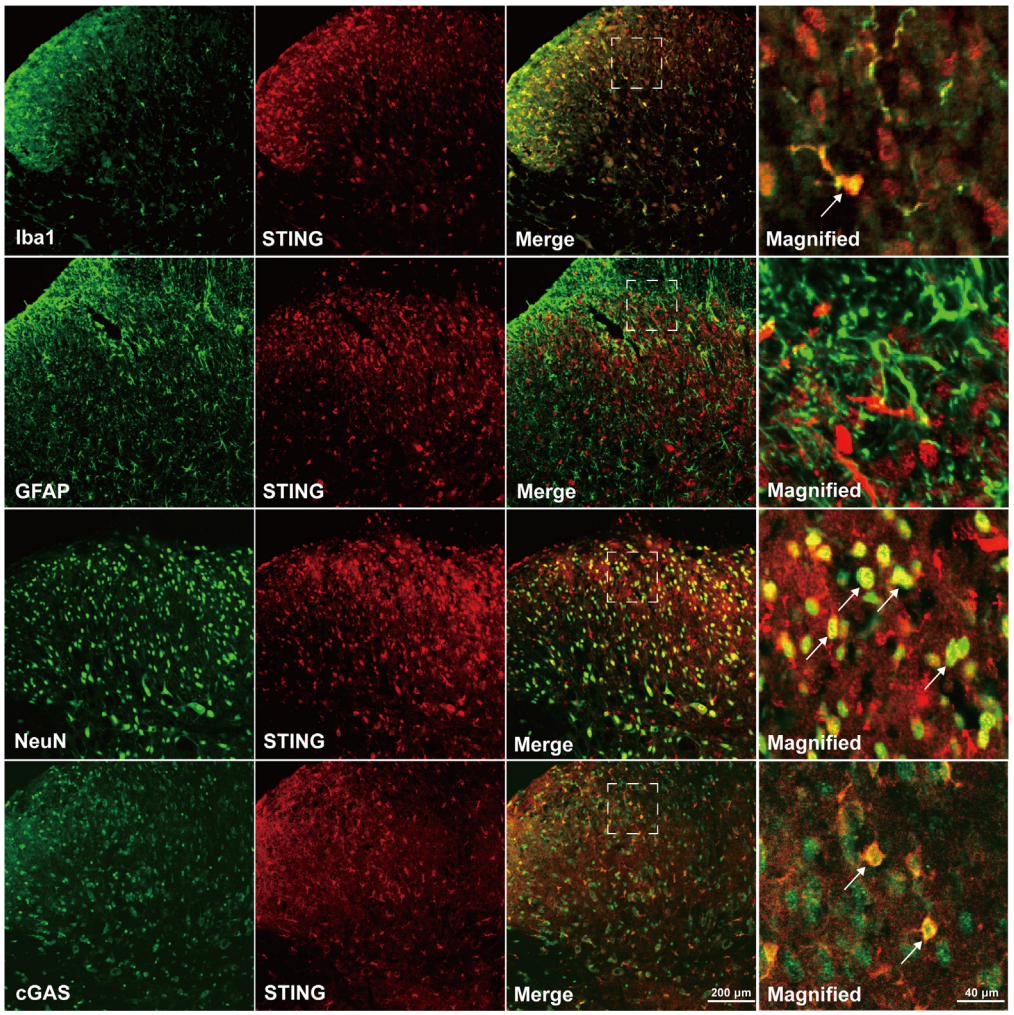

Figure 3. Colocalization of STING with NeuN, Iba1, and cGAS in the spinal dorsal horn

Double immunofluorescence staining showed that STING colocalized with NeuN and Iba1 but not GFAP. STING also colocalized with cGAS. NeuN, neuron-specific nuclear protein; GFAP, glial fibrillary acidic protein; Iba1, ionized calcium-binding adaptor molecule-1. White arrows indicate colocalization.

expression (~40%) in the spinal dorsal horn (Figure 5B; $^{**}p < 0.01$, vs. Polyethylenimine (PEI), one-way ANOVA, n = 3). Therefore, TAOK2-siRNA (10 μg) was used in the following experiments. Western blot and behavioral tests showed that, while the spinal TAOK2 expression and phosphorylation were reduced by TAOK2-siRNA (Figures 5C and 5D; $^{**}p < 0.01$, $^{***}p < 0.001$, vs. CCI+PEI, one-way ANOVA, n = 4), the MWT significantly increased and ATS significantly decreased in the CCI+siRNA group from days 9 to 14 after CCI (Figures 5E and 5F; $^{*}p < 0.05$, $^{**}p < 0.01$, $^{***}p < 0.001$, vs. CCI+PEI, two-way ANOVA, n = 7), compared with those in the CCI+PEI group, suggesting that TAOK2 in the spinal dorsal horn plays an important role in the maintenance of neuropathic pain. To further investigate the molecular mechanism of TAOK2-mediated neuropathic pain, we measured the expression of cGAS and STING after intrathecal application of TAOK2-siRNA. The results showed that compared with that in the CCI+PEI group, the expression of cGAS and STING significantly decreased in the CCI+-siRNA group (Figures 5G and 5H; $^{**}p < 0.01$, $^{***}p < 0.001$, vs. CCI+PEI, one-way ANOVA, n = 4), which demonstrated that the cGAS-STING signaling pathway might be the downstream target of TAOK2-mediated neuropathic pain in the spinal dorsal horn.

TAOK2 activation induced hyperalgesia and activated cGAS-STING in naive rats

To explore the role of TAOK2 phosphorylation in neuropathic pain, nocodazole, a specific TAOK2 agonist, was injected intrathecally into naive rats. Behavioral results showed that compared with those in the DMSO group, the MWT significantly decreased and ATS significantly increased in the nocodazole group (Figures 6A and 6B; $^{***}p < 0.001$, vs. DMSO, one-way ANOVA, n = 7), which suggested that TAOK2 phosphorylation in the spinal dorsal horn contributed to hyperalgesia in naive rats. Western blot analysis showed no significant differences in the expression of TAOK2 among the three groups (Figure 6C). Compared with those in the DMSO group, the phosphorylation level of TAOK2 and the expression of cGAS and STING significantly increased in the nocodazole group (Figures 6D–6F; $^{**}p < 0.01$, $^{***}p < 0.001$, vs. DMSO,

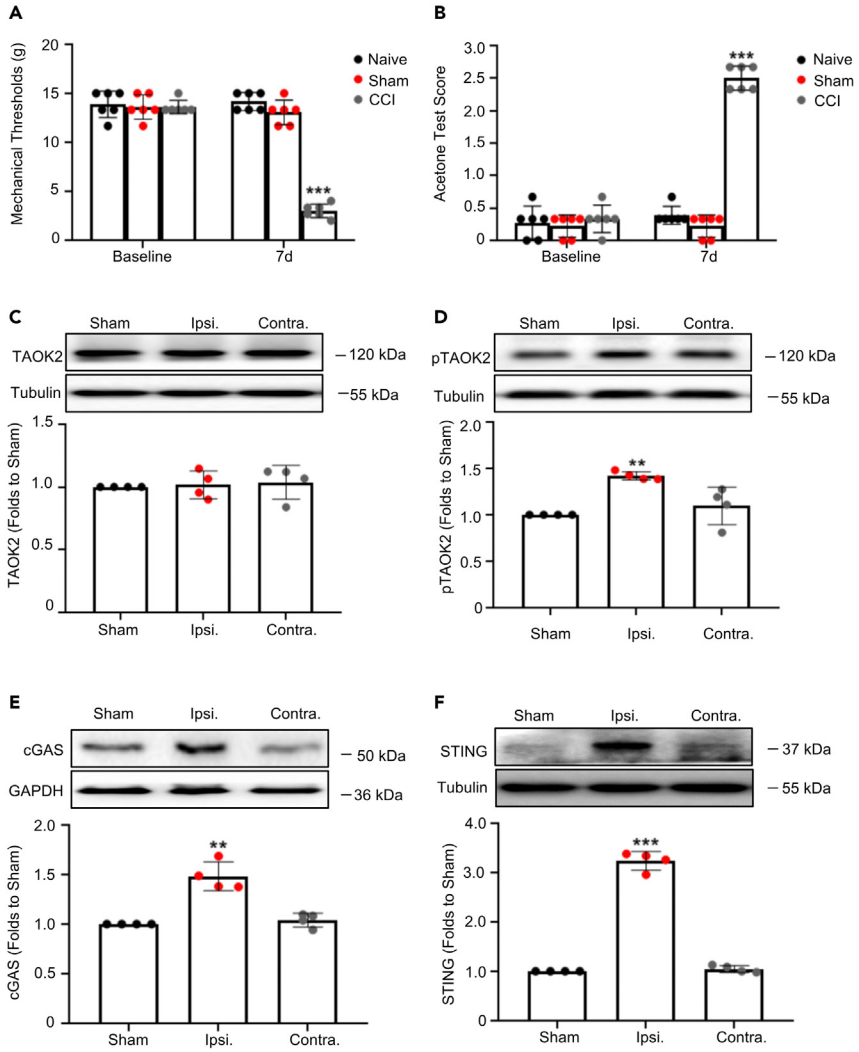

Figure 4. CCI-induced behavioral hyperalgesia and activation of TAOK2 and cGAS-STING signaling

(A and B) The CCI group showed significantly lower MWT (A) and higher ATS (B) than did the sham group on the 7th day after surgery (***p < 0.001, one-way ANOVA, n = 7).

(C) Western blotting showed that, compared to that in the sham group, the total abundance of TAOK2 did not change in the CCI group.

(D) Compared to that in the sham group, the phosphorylation level of TAOK2 was significantly increased in the ipsilateral spinal dorsal horn of the CCI group (**p < 0.01, vs. sham, one-way ANOVA, n = 4).

(E and F) Compared to that in the sham group, the expression of cGAS (E) and STING (F) was significantly upregulated in the ipsilateral spinal dorsal horn of the CCI group (**p < 0.01, ***p < 0.001, vs. Sham, one-way ANOVA, n = 4). Error bars represent the SEM.

one-way ANOVA, n = 4). Moreover, the expression of cGAS and STING was reduced in the nocodazole + TAOK2-siRNA group compared to that in the nocodazole + PEI group (Figures 6G and 6H; *p < 0.05, **p < 0.01, vs. nocodazole + PEI, one-way ANOVA, n = 3), ruling out the direct activation of cGAS-STING by nocodazole. These data suggest that nocodazole activates TAOK2 and that the cGAS-STING signaling pathway is the potential downstream target of TAOK2 activation-mediated hyperalgesia.

Inhibition of cGAS-STING reversed behavioral hyperalgesia induced by CCI

To further explore whether the cGAS-STING signaling pathway in the spinal dorsal horn plays an independent role in neuropathic pain, the cGAS inhibitor RU.521 or STING inhibitor C-176 was injected intrathecally on days 7 and 8 after CCI. The behavioral test results showed that both RU.521 and C-176 significantly increased the MWT and decreased the ATS induced by CCI when compared with those in the DMSO group (Figures 7A and 7B; **p < 0.01, ***p < 0.001, C-176 vs. DMSO; ##p < 0.01, ###p < 0.001, RU.521 vs. DMSO, two-way ANOVA, n = 7), suggesting that the inhibition of cGAS or STING alleviated hyperalgesia in CCI rats. These results indicated that the cGAS-STING signaling

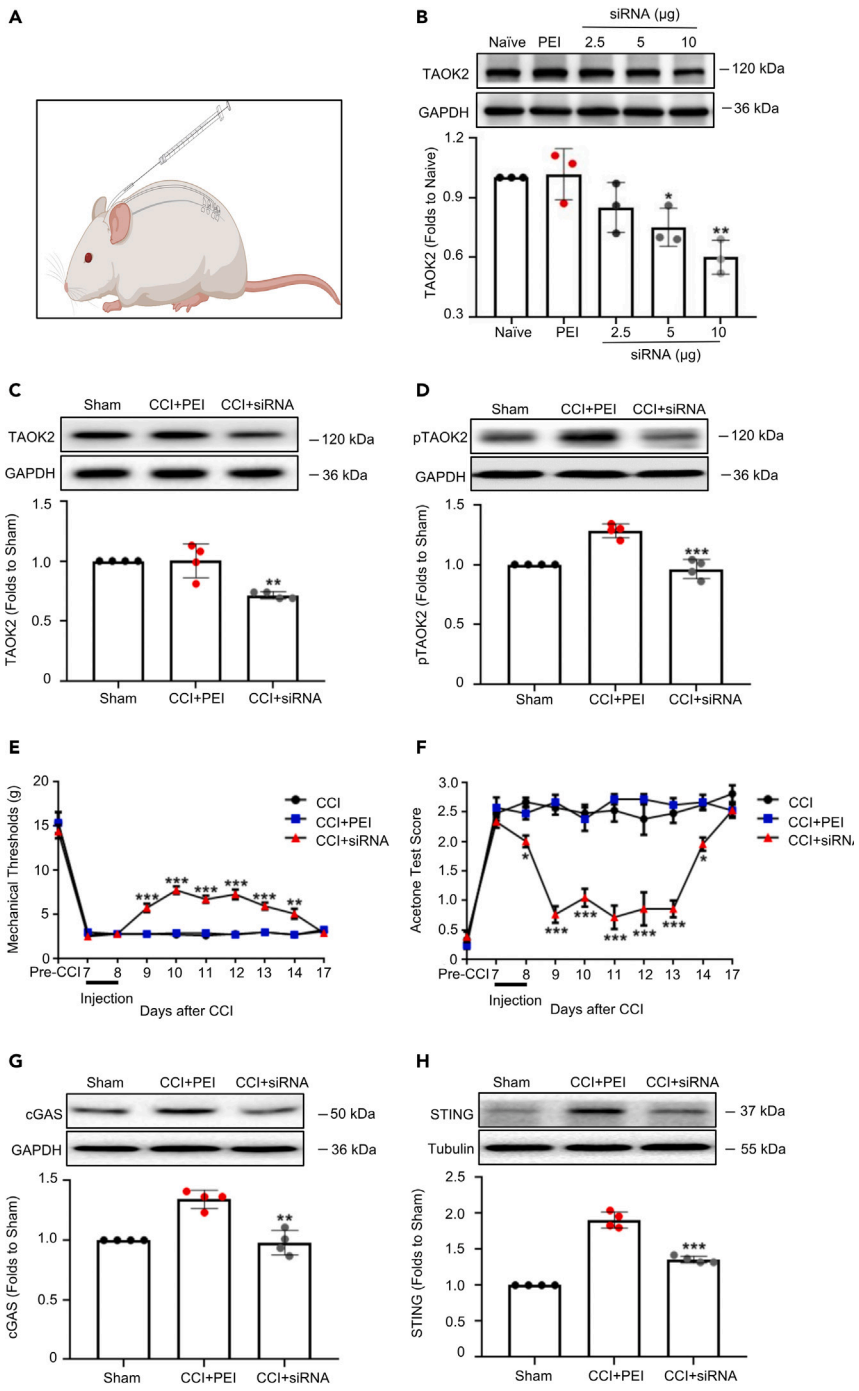

Figure 5. Silencing TAOK2 reversed the behavioral hyperalgesia and suppressed the upregulation of cGAS-STING induced by CCI

(A) A schematic diagram of the experiments.

(B) Compared with that in the PEI group, the expression level of TAOK2 was significantly decreased in the siRNA (10 μg) group (**p < 0.01, vs. PEI, one-way ANOVA, n = 3).

(C and D) Compared to those in the CCI+PEI group, the total abundance of TAOK2 (C) and its phosphorylation level (D) were significantly decreased in the CCI+siRNA group (**p < 0.01, ***p < 0.001, vs. CCI+PEI, one-way ANOVA, n = 4).

(E) Compared to that in the CCI+PEI group, the MWT significantly increased in the CCI+siRNA group from days 9 to 14 after CCI (**p < 0.01, ***p < 0.001, vs. CCI+PEI, two-way ANOVA, n = 7).

Figure 5. *Continued*

(F) Compared to that in the CCI+PEI group, the ATS significantly decreased in the CCI+siRNA group from days 9 to 14 after CCI (*p < 0.05, ***p < 0.001, vs. CCI+PEI, two-way ANOVA, n = 7).

(G and H) Compared to that in the CCI+PEI group, the expression of cGAS (G) and STING (H) was significantly downregulated in the CCI+siRNA group (**p < 0.01, ***p < 0.001, vs. CCI+PEI, one-way ANOVA, n = 4). Error bars represent the SEM.

pathway in the spinal dorsal horn plays an independent role in neuropathic pain. Western blot results showed that compared with DMSO, neither RU.521 nor C-176 had a significant effect on the expression level of TAOK2 or its phosphorylation and the expression of cGAS in the spinal dorsal horn (Figures 7C–7E). However, STING expression significantly decreased in the RU.521 group (Figure 7F; **p < 0.01, vs. DMSO, one-way ANOVA, n = 4). These results suggested that TAOK2 is the upstream target of cGAS-STING and that STING is the downstream molecule of cGAS in the spinal dorsal horn

Knockdown of STING impeded initiation of neuropathic pain after CCI

To further confirm the role of STING in neuropathic pain, we performed an intrathecal application of AAV-shRNA-STING to knock down the expression of STING in the spinal dorsal horn. CCI surgery was performed 3 weeks after the intrathecal injection of AAV-shRNA-STING. The ipsilateral spinal dorsal horn was harvested to detect the viral transfection efficiency and STING expression. The results showed that the enhanced green fluorescent protein was expressed clearly in the spinal dorsal horn (Figure 8A), and compared with that in the AAV-control group, the expression level of STING in the spinal dorsal horn in the AAV-STING group significantly decreased (Figure 8B; ***p < 0.001, vs. CCI+AAV-Control, one-way ANOVA, n = 4), indicating the successful transfection and knockdown of STING protein. Behavioral tests showed that, compared with those in the AAV-control group, the MWT significantly increased and the ATS significantly decreased on days 7, 8, and 9 after CCI (Figures 8C and 8D; *p < 0.05, **p < 0.01, ***p < 0.001, vs. CCI+AAV-Control, two-way ANOVA, n = 7), suggesting that STING in the spinal dorsal horn played a promoting role in the development of neuropathic pain.

DISCUSSION

To the best of our knowledge, this study provides the first piece of evidence showing that spinal TAOK2 contributes to the development of neuropathic pain via activation of cGAS-STING signaling. Consistent with the hyperalgesia induced by CCI, TAOK2, as well as the cGAS-STING signaling pathway, was activated, while silencing TAOK2 or inhibiting cGAS-STING alleviated behavioral hyperalgesia and inhibited protein expression, suggesting that spinal TAOK2 and cGAS-STING signaling are involved in the maintenance of neuropathic pain.

The spinal dorsal horn is the primary relay station and is responsible for processing nociceptive signals from peripheral sensation to the central nervous system.[32–34] Misregulation of neurotransmitter release and synaptic plasticity is critical for the initiation and development of neuropathic pain.[35,36] Studies revealed that TAOK2 plays an important role in cellular mitosis, cytoskeleton formation, tumor cell differentiation,[37] and is involved in the development of autism and schizophrenia.[17,18,38,39] More importantly, a recent study demonstrated that TAOK2 modulates the responsiveness to mechanical stimuli by regulating the expression and localization of mechanical stimulation-related receptors in *Drosophila* neurons,[21] providing a critical clue for its potential role in pain modulation in mammals. However, there are no reports on the association of TAOK2 with hyperalgesia induced by neuropathic pain.

In the present study, gene silencing was employed to explore the role of spinal TAOK2 in a rat neuropathic pain model. Western blotting showed that TAOK2-siRNA significantly reduced the expression and phosphorylation level of TAOK2 in the spinal dorsal horn. Meanwhile, behavioral results showed that TAOK2-siRNA significantly alleviated mechanical and cold hyperalgesia in CCI rats, demonstrating that TAOK2 plays an important role in the maintenance of neuropathic pain. Further experiment showed that after the administration of TAOK2-siRNA, the protein expression of cGAS and STING in the spinal dorsal horn was significantly reduced, suggesting that the downstream molecular mechanism of TAOK2 involves the cGAS-STING signaling pathway in the spinal dorsal horn. To investigate whether activation of spinal TAOK2 sufficiently induces hyperalgesia as suggested in the literature,[40,41] we injected a specific agonist of TAOK2, nocodazole, into the subarachnoid space of naive rats. Western blotting showed that nocodazole had no significant effect on the total expression, but notably increased the phosphorylation level of TAOK2. Meanwhile, behavioral tests showed that nocodazole induced hyperalgesia via both mechanical and cold stimuli, suggesting that the activation of spinal TAOK2 sufficiently induces behavioral hyperalgesia. To rule out the possibility of direct activation of cGAS or STING by nocodazole, we used nocodazole in *taok2*-silenced animals. The results showed that TAOK2-siRNA blocked the effect of nocodazole on cGAS and STING, implying that TAOK2 mediates nocodazole-induced cGAS-STING activation.

Previous studies have revealed that the cGAS-STING signaling pathway is involved in neurological degenerative disorders.[42–44] Recent studies reported that the activity of STING mediates neuropathic pain by regulating the inflammatory factor interleukin-6, and pharmacological inhibition of cGAS-STING signaling attenuated neuropathic pain by suppressing the activation of interferon regulatory factor 3[30,31]. By contrast, other studies have found that STING activity is negatively correlated with pain behaviors.[29,45] In the present study, to further investigate the role of cGAS-STING signaling in CCI-induced neuropathic pain, we either intrathecally injected cGAS- or STING-specific inhibitors or shRNA to downregulate the function of cGAS-STING signaling. Behavioral results showed that both the cGAS and STING inhibitors and knockdown of STING alleviated behavioral hyperalgesia, suggesting that the cGAS-STING signaling pathway in the spinal dorsal horn facilitates the development of neuropathic pain. Western blotting results showed that intrathecal injection of cGAS or STING inhibitor did not change the expression and phosphorylation levels of TAOK2, indicating that TAOK2 is an upstream signaling molecule of cGAS-STING signaling.

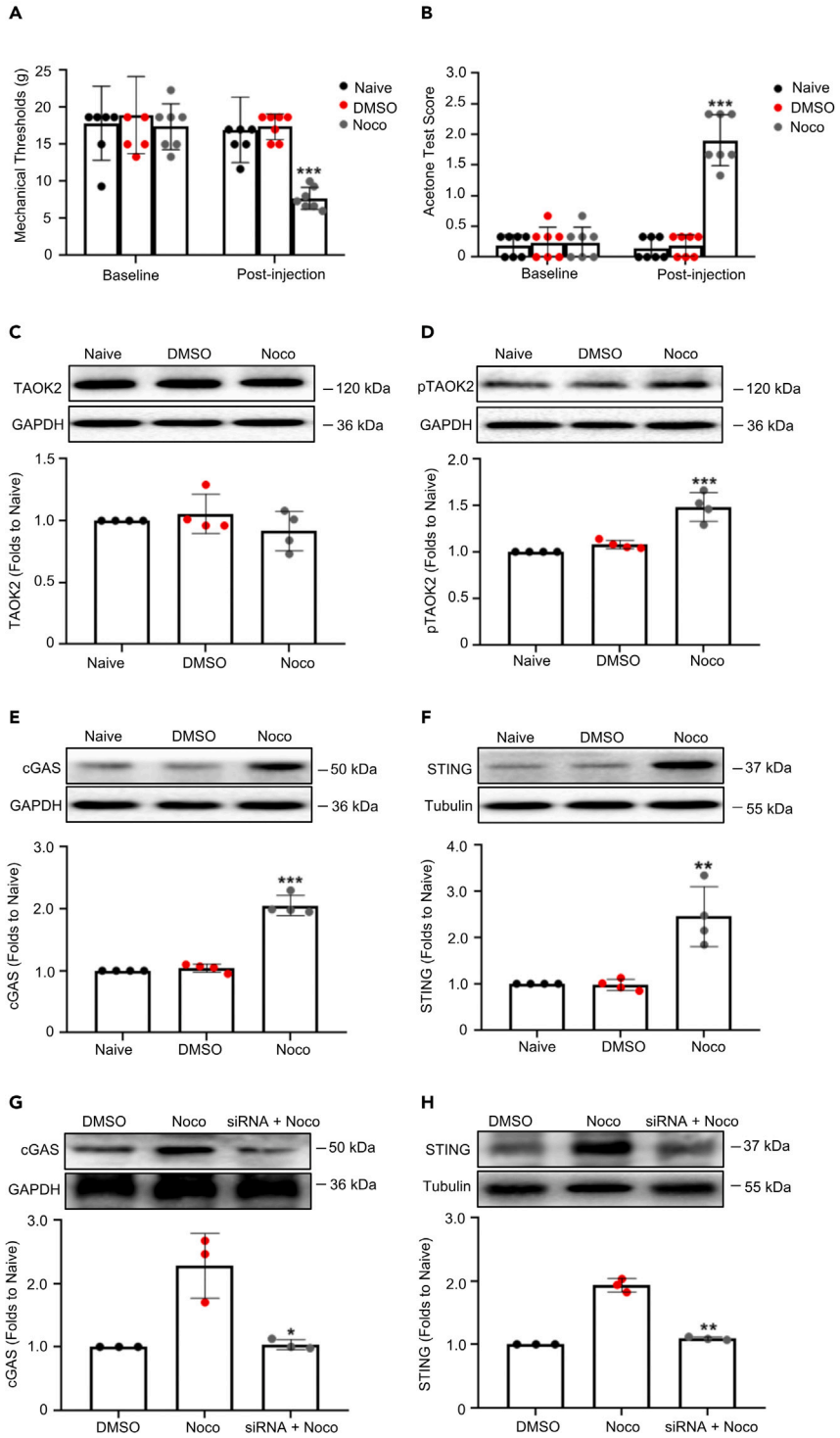

Figure 6. Activation of TAOK2 induced behavioral hyperalgesia and activated cGAS-STING in naive rats

(A and B) The nocodazole group showed significantly lower MWT (A) and higher ATS (B) after drug administration than did the DMSO group (***$p < 0.001$, one-way ANOVA, n = 7).

(C) The expression of TAOK2 showed no significant differences among the three groups.

(D) Compared with that in the DMSO group, the phosphorylation level of TAOK2 significantly increased in the nocodazole group (***$p < 0.001$, vs. DMSO, one-way ANOVA, n = 4).

Figure 6. *Continued*

(E and F) Compared with that in the DMSO group, the expression of cGAS (E) and STING (F) was significantly upregulated in the nocodazole group (**p < 0.01, ***p < 0.001, vs. DMSO, one-way ANOVA, n = 4).

(G and H) Moreover, compared to that in the nocodazole + PEI group, the expression of cGAS (G) and STING (H) was significantly decreased in the nocodazole + TAOK2-siRNA group (*p < 0.05, **p < 0.01, vs. nocodazole + PEI, one-way ANOVA, n = 3). Error bars represent the SEM.

In the present study, we found that TAOK2 mediates neuropathic pain by regulating the cGAS-STING signaling pathway. However, the exact mechanism remains to be investigated. Among a variety of neurotransmitters, glutamate is a vital excitatory neurotransmitter released by afferent signals to transduce information.[46–49] Disturbance of glutamate release or receptor dysfunction has been proven to be involved in the development of neuropathic pain.[50–52] It is reported that in hippocampal neurons, TAOK2 regulates NMDAR-mediated Ca^{2+} influx,[36] while mitochondrial oxidative stress increases intracellular DNA fragments, which may contribute to the development of neuropathic

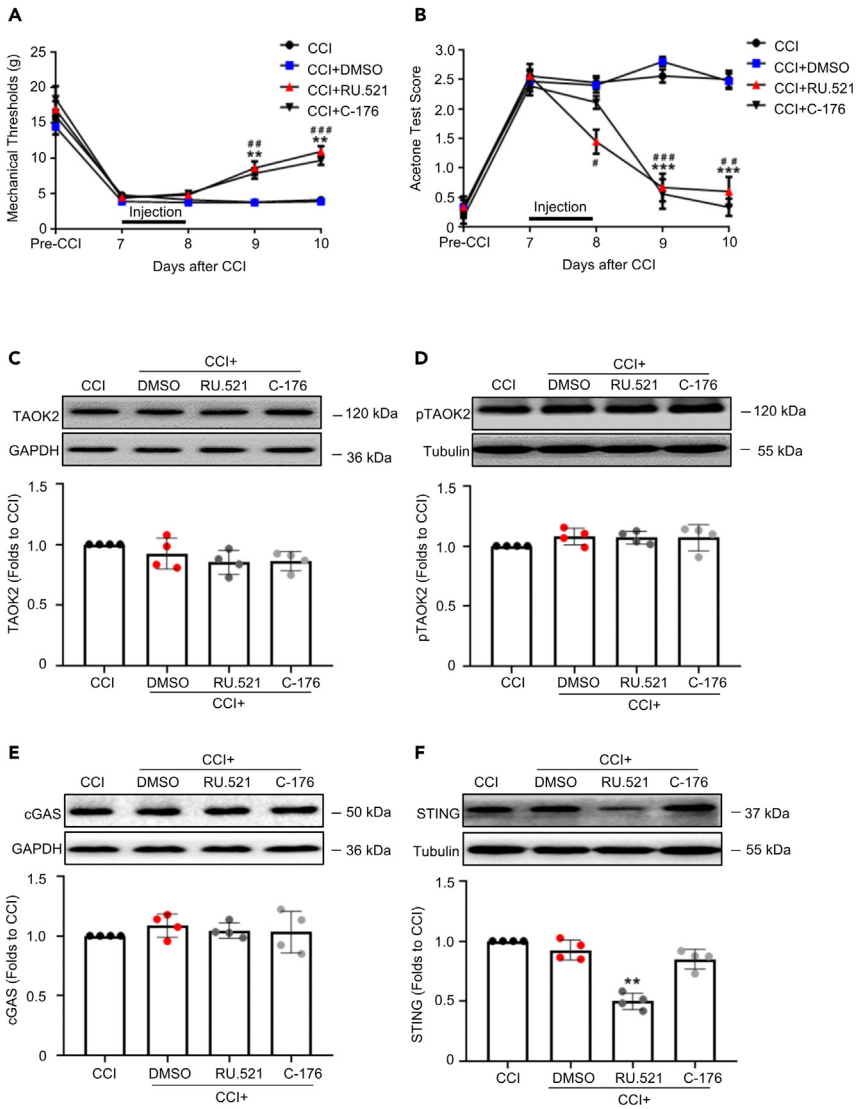

Figure 7. Inhibition of cGAS-STING reversed behavioral hyperalgesia induced by CCI

(A) Compared with that in the CCI+DMSO group, the MWT significantly increased in the CCI+ RU.521 and CCI+C-176 groups on days 9 and 10 after CCI (**p < 0.01, C-176 vs. DMSO; $^{\#\#}$p < 0.01, $^{\#\#\#}$p < 0.001, RU.521 vs. DMSO, two-way ANOVA, n = 7).

(B) Compared with that in the CCI+DMSO group, the ATS significantly decreased in the CCI+ RU.521 and CCI+C-176 groups on days 8, 9, and 10 after CCI (***p < 0.001, C-176 vs. DMSO; $^{\#}$p < 0.05, $^{\#\#}$p < 0.01, $^{\#\#\#}$p < 0.001, RU.521 vs. DMSO, two-way ANOVA, n = 7).

(C and D) The expression of TAOK2 (C), phosphorylated TAOK2 (D), and cGAS (E) showed no significant differences in each group.

(F) The expression of STING was significantly lower in the CCI+RU.521 group than in the CCI+DMSO group (**p < 0.01, vs. DMSO, one-way ANOVA, n = 4). Error bars represent the SEM.

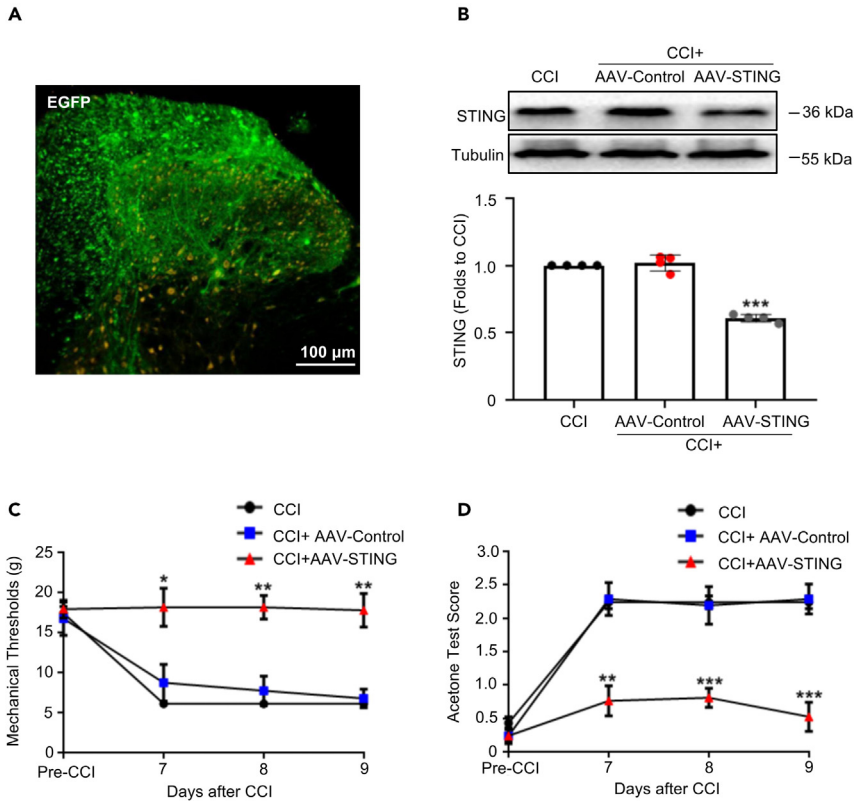

Figure 8. Knockdown of STING impeded the initiation of neuropathic pain after CCI

(A) Enhanced green fluorescent protein was expressed in the spinal dorsal horn 3 weeks after transfection.

(B) Compared to that in the CCI+AAV-Control group, the expression of STING significantly decreased in the CCI+AAV-STING group (***$p < 0.001$, vs. CCI+AAV-Control, one-way ANOVA, n = 4).

(C) Compared with that in the AAV-control group, the MWT significantly increased on days 7, 8, and 9 after CCI (*$p < 0.05$, **$p < 0.01$, vs. CCI+AAV-Control, two-way ANOVA, n = 7).

(D) Compared with that in the AAV-control group, the ATS significantly decreased on days 7, 8, and 9 after CCI (**$p < 0.01$, ***$p < 0.001$, vs. CCI+AAV-Control, two-way ANOVA, n = 7). Error bars represent the SEM. EGFP, enhanced green fluorescent protein.

pain.[53–56] Taken together, it might be inferred that the spinal cGAS-STING signaling pathway is activated by stress induced by CCI and then activates downstream signaling to promote the development of neuropathic pain. However, further investigation is required to determine whether spinal TAOK2 directly affects excitatory transmission and thereby activates the cGAS-STING signaling pathway to mediate neuropathic pain.

In conclusion, the present study revealed that spinal TAOK2 mediates neuropathic pain by regulating the activity of the cGAS-STING signaling pathway, suggesting a vital role for TAOK2 in the development of neuropathic pain and providing new molecular targets for basic medicine and clinical treatment of neuropathic pain.

Limitations of the study

This study provided evidence for the critical role of spinal TAOK2 activation in the maintenance of neuropathic pain. However, the relationship between spinal TAOK2 and neuronal cGAS-STING signaling activation remains to be further elucidated, which leads to an obvious limitation in understanding the underlying mechanism. Due to technical reasons, we were unable to detect the mRNA localization of these molecules by *in situ* hybridization or perform neurotransmitter release studies, which are important for revealing or validating the link between signaling molecules and obtaining a comprehensive understanding of the synaptic or cellular mechanisms underlying neuropathic pain.

STAR★METHODS

Detailed methods are provided in the online version of this paper and include the following:

- KEY RESOURCES TABLE
- RESOURCE AVAILABILITY
  - Lead contact

ACKNOWLEDGMENTS

This research was supported by the Natural Science Foundation of Zhejiang Province, China (LZ21H090001, LBY22H270007, and LR23C090001), the National Natural Science Foundation of China (32071019), and the STI2030-Major Projects (2021ZD0200408).

AUTHOR CONTRIBUTIONS

Conceptualization, Y.-X.Y. and Y.Y.; Methodology, H.Z., A.L., and Y.-F.L.; Validation, J.-P.L. and Y.-X.Y.; Investigation, Z.-M.S., B.-X.J., and Y.-X.Y.; Writing – Original Draft, A.L. and H.Z.; Writing – Review and Editing, A.L., H.Z., and Y.-X.Y.; Funding Acquisition, Y.Y. and Y.-X.Y.; Supervision, Y.-X.Y. The authors read and approved the final manuscript.

DECLARATION OF INTERESTS

The authors declare no competing interests.

Received: October 18, 2022
Revised: May 25, 2023
Accepted: August 29, 2023
Published: August 30, 2023

REFERENCES

1. Cohen, S.P., and Mao, J. (2014). Neuropathic pain: mechanisms and their clinical implications. BMJ *348*, f7656. https://doi.org/10.1136/bmj.f7656.
2. Finnerup, N.B., Haroutounian, S., Kamerman, P., Baron, R., Bennett, D.L.H., Bouhassira, D., Cruccu, G., Freeman, R., Hansson, P., Nurmikko, T., et al. (2016). Neuropathic pain: an updated grading system for research and clinical practice. Pain *157*, 1599–1606. https://doi.org/10.1097/j.pain.0000000000000492.
3. Cohen, S.P., Vase, L., and Hooten, W.M. (2021). Chronic pain: an update on burden, best practices, and new advances. Lancet *397*, 2082–2097. https://doi.org/10.1016/S0140-6736(21)00393-7.
4. Ishikawa, T., Murata, K., Okuda, H., Potapenko, I., Hori, K., Furuyama, T., Yamamoto, R., Ono, M., Kato, N., Fukazawa, Y., and Ozaki, N. (2023). Pain-related neuronal ensembles in the primary somatosensory cortex contribute to hyperalgesia and anxiety. iScience *26*, 106332. https://doi.org/10.1016/j.isci.2023.106332.
5. Liang, L.L., Yang, J.L., Lü, N., Gu, X.Y., Zhang, Y.Q., and Zhao, Z.Q. (2010). Synergetic analgesia of propentofylline and electroacupuncture by interrupting spinal glial function in rats. Neurochem. Res. *35*, 1780–1786. https://doi.org/10.1007/s11064-010-0244-x.
6. Attal, N., and Bouhassira, D. (2021). Advances in the treatment of neuropathic pain. Curr. Opin. Neurol. *34*, 631–637. https://doi.org/10.1097/WCO.0000000000000980.
7. Ji, R.R., Donnelly, C.R., and Nedergaard, M. (2019). Astrocytes in chronic pain and itch. Nat. Rev. Neurosci. *20*, 667–685. https://doi.org/10.1038/s41583-019-0218-1.
8. Gangadharan, V., Zheng, H., Taberner, F.J., Landry, J., Nees, T.A., Pistolic, J., Agarwal, N., Männich, D., Benes, V., Helmstaedter, M., et al. (2022). Neuropathic pain caused by miswiring and abnormal end organ targeting. Nature *606*, 137–145. https://doi.org/10.1038/s41586-022-04777-z.
9. Kahle, K.T., Schmouth, J.F., Lavastre, V., Latremoliere, A., Zhang, J., Andrews, N., Omura, T., Laganière, J., Rochefort, D., Hince, P., et al. (2016). Inhibition of the kinase WNK1/HSN2 ameliorates neuropathic pain by restoring GABA inhibition. Sci. Signal. *9*, ra32. https://doi.org/10.1126/scisignal.aad0163.
10. Wang, F., Ma, S.B., Tian, Z.C., Cui, Y.T., Cong, X.Y., Wu, W.B., Wang, F.D., Li, Z.Z., Han, W.J., Wang, T.Z., et al. (2021). Nociceptor-localized cGMP-dependent protein kinase I is a critical generator for central sensitization and neuropathic pain. Pain *162*, 135–151. https://doi.org/10.1097/j.pain.0000000000002013.
11. Fu, Y.Y., Cen, J.K., Song, H.L., Song, S.Y., Zhang, Z.J., and Lu, H.J. (2022). Ginsenoside Rh2 Ameliorates Neuropathic Pain by inhibition of the miRNA21-TLR8-mitogen-activated protein kinase axis. Mol. Pain *18*, 17448069221126078. https://doi.org/10.1177/17448069221126078.
12. Moore, T.M., Garg, R., Johnson, C., Coptcoat, M.J., Ridley, A.J., and Morris, J.D. (2000). PSK, a novel STE20-like kinase derived from prostatic carcinoma that activates the c-Jun N-terminal kinase mitogen-activated protein kinase pathway and regulates actin cytoskeletal organization. J. Biol. Chem. *275*, 4311–4322. https://doi.org/10.1074/jbc.275.6.4311.
13. Chen, Z., Hutchison, M., and Cobb, M.H. (1999). Isolation of the protein kinase TAO2 and identification of its mitogen-activated protein kinase/extracellular signal-regulated kinase kinase binding domain. J. Biol. Chem. *274*, 28803–28807. https://doi.org/10.1074/jbc.274.40.28803.
14. Timm, T., Li, X.Y., Biernat, J., Jiao, J., Mandelkow, E., Vandekerckhove, J., and Mandelkow, E.M. (2003). MARKK, a Ste20-like kinase, activates the polarity-inducing kinase MARK/PAR-1. EMBO J. *22*, 5090–5101. https://doi.org/10.1093/emboj/cdg447.
15. Raman, M., Earnest, S., Zhang, K., Zhao, Y., and Cobb, M.H. (2007). TAO kinases mediate activation of p38 in response to DNA damage. EMBO J. *26*, 2005–2014. https://doi.org/10.1038/sj.emboj.7601668.
16. Yasuda, S., Tanaka, H., Sugiura, H., Okamura, K., Sakaguchi, T., Tran, U., Takemiya, T., Mizoguchi, A., Yagita, Y., Sakurai, T., et al. (2007). Activity-induced protocadherin arcadlin regulates dendritic spine number by triggering N-cadherin endocytosis via TAO2beta and p38 MAP kinases. Neuron *56*,

456–471. https://doi.org/10.1016/j.neuron.2007.08.020.
17. Richter, M., Murtaza, N., Scharrenberg, R., White, S.H., Johanns, O., Walker, S., Yuen, R.K.C., Schwanke, B., Bedürftig, B., Henis, M., et al. (2019). Altered TAOK2 activity causes autism-related neurodevelopmental and cognitive abnormalities through RhoA signaling. Mol. Psychiatr. *24*, 1329–1350. https://doi.org/10.1038/s41380-018-0025-5.
18. Willis, A., Pratt, J.A., and Morris, B.J. (2021). BDNF and JNK signaling modulate cortical interneuron and perineuronal net development: implications for schizophrenia-linked 16p11.2 duplication syndrome. Schizophr. Bull. *47*, 812–826. https://doi.org/10.1093/schbul/sbaa139.
19. Tavares, I.A., Touma, D., Lynham, S., Troakes, C., Schober, M., Causevic, M., Garg, R., Noble, W., Killick, R., Bodi, I., et al. (2013). Prostate-derived sterile 20-like kinases (PSKs/TAOKs) phosphorylate tau protein and are activated in tangle-bearing neurons in Alzheimer disease. J. Biol. Chem. *288*, 15418–15429. https://doi.org/10.1074/jbc.M112.448183.
20. Giacomini, C., Koo, C.Y., Yankova, N., Tavares, I.A., Wray, S., Noble, W., Hanger, D.P., and Morris, J.D.H. (2018). A new TAO kinase inhibitor reduces tau phosphorylation at sites associated with neurodegeneration in human tauopathies. Acta Neuropathol Com *6*, 37. https://doi.org/10.1186/s40478-018-0539-8.
21. Hu, C., Kanellopoulos, A.K., Richter, M., Petersen, M., Konietzny, A., Tenedini, F.M., Hoyer, N., Cheng, L., Poon, C.L.C., Harvey, K.F., et al. (2020). Conserved tao kinase activity regulates dendritic arborization, cytoskeletal dynamics, and sensory function in Drosophila. J. Neurosci. *40*, 1819–1833. https://doi.org/10.1523/JNEUROSCI.1846-19.2020.
22. Areti, A., Yerra, V.G., Komirishetty, P., and Kumar, A. (2016). Potential therapeutic benefits of maintaining mitochondrial health in peripheral neuropathies. Curr. Neuropharmacol. *14*, 593–609. https://doi.org/10.2174/1570159x14666151126215358.
23. Fehrenbacher, J.C., Guo, C., Kelley, M.R., and Vasko, M.R. (2017). DNA damage mediates changes in neuronal sensitivity induced by the inflammatory mediators, Mcp-1 and LPS, and can be reversed by enhancing the DNA repair function of Ape1. Neuroscience *366*, 23–35. https://doi.org/10.1016/j.neuroscience.2017.09.039.
24. Lai, C.Y., Hsieh, M.C., Ho, Y.C., Lee, A.S., Wang, H.H., Cheng, J.K., Chau, Y.P., and Peng, H.Y. (2017). Growth arrest and DNA-damage-inducible protein 45beta-mediated DNA demethylation of voltage-dependent T-type calcium channel 3.2 subunit enhances neuropathic allodynia after nerve injury in rats. Anesthesiology *126*, 1077–1095. https://doi.org/10.1097/ALN.0000000000001610.
25. Zhang, X., Wu, J., Du, F., Xu, H., Sun, L., Chen, Z., Brautigam, C.A., Zhang, X., and Chen, Z.J. (2014). The cytosolic DNA sensor cGAS forms an oligomeric complex with DNA and undergoes switch-like conformational changes in the activation loop. Cell Rep. *6*, 421–430. https://doi.org/10.1016/j.celrep.2014.01.003.
26. Zhang, X., Shi, H., Wu, J., Zhang, X., Sun, L., Chen, C., and Chen, Z.J. (2013). Cyclic GMP-AMP containing mixed phosphodiester linkages is an endogenous high-affinity ligand for STING. Mol. Cell *51*, 226–235. https://doi.org/10.1016/j.molcel.2013.05.022.
27. Srikanth, S., Woo, J.S., Wu, B., El-Sherbiny, Y.M., Leung, J., Chupradit, K., Rice, L., Seo, G.J., Calmettes, G., Ramakrishna, C., et al. (2019). The Ca^{2+} sensor STIM1 regulates the type I interferon response by retaining the signaling adaptor STING at the endoplasmic reticulum. Nat. Immunol. *20*, 152–162. https://doi.org/10.1038/s41590-018-0287-8.
28. Liu, S., Cai, X., Wu, J., Cong, Q., Chen, X., Li, T., Du, F., Ren, J., Wu, Y.T., Grishin, N.V., and Chen, Z.J. (2015). Phosphorylation of innate immune adaptor proteins MAVS, STING, and TRIF induces IRF3 activation. Science *347*, aaa2630. https://doi.org/10.1126/science.aaa2630.
29. Donnelly, C.R., Jiang, C., Andriessen, A.S., Wang, K., Wang, Z., Ding, H., Zhao, J., Luo, X., Lee, M.S., Lei, Y.L., et al. (2021). STING controls nociception via type I interferon signalling in sensory neurons. Nature *591*, 275–280. https://doi.org/10.1038/s41586-020-03151-1.
30. Sun, J., Zhou, Y.Q., Xu, B.Y., Li, J.Y., Zhang, L.Q., Li, D.Y., Zhang, S., Wu, J.Y., Gao, S.J., Ye, D.W., and Mei, W. (2022). STING/NF-kappaB/IL-6-mediated inflammation in microglia contributes to spared nerve injury (SNI)-induced pain initiation. J. Neuroimmune Pharmacol. *17*, 453–469. https://doi.org/10.1007/s11481-021-10031-6.
31. Wu, W., Zhang, X., Wang, S., Li, T., Hao, Q., Li, S., Yao, W., and Sun, R. (2022). Pharmacological inhibition of the cGAS-STING signaling pathway suppresses microglial M1-polarization in the spinal cord and attenuates neuropathic pain. Neuropharmacology *217*, 109206. https://doi.org/10.1016/j.neuropharm.2022.109206.
32. Chu, Y.X., Zhang, Y., Zhang, Y.Q., and Zhao, Z.Q. (2010). Involvement of microglial P2X7 receptors and downstream signaling pathways in long-term potentiation of spinal nociceptive responses. Brain Behav. Immun. *24*, 1176–1189. https://doi.org/10.1016/j.bbi.2010.06.001.
33. Smith, K.M., and Ross, S.E. (2020). Making connections: recent advances in spinal cord dorsal horn circuitry. Pain *161* (*Suppl 1*), S122–S126. https://doi.org/10.1097/j.pain.0000000000001980.
34. Li, L., Bai, L., Yang, K., Zhang, J., Gao, Y., Jiang, M., Yang, Y., Zhang, X., Wang, L., Wang, X., et al. (2021). KDM6B epigenetically regulated-interleukin-6 expression in the dorsal root ganglia and spinal dorsal horn contributes to the development and maintenance of neuropathic pain following peripheral nerve injury in male rats. Brain Behav. Immun. *98*, 265–282. https://doi.org/10.1016/j.bbi.2021.08.231.
35. Alles, S.R.A., and Smith, P.A. (2018). Etiology and pharmacology of neuropathic pain. Pharmacol. Rev. *70*, 315–347. https://doi.org/10.1124/pr.117.014399.
36. Peirs, C., Dallel, R., and Todd, A.J. (2020). Recent advances in our understanding of the organization of dorsal horn neuron populations and their contribution to cutaneous mechanical allodynia. J. Neural. Transm. *127*, 505–525. https://doi.org/10.1007/s00702-020-02159-1.
37. Ye, J., Shi, M., Chen, W., Zhu, F., and Duan, Q. (2020). Research advances in the molecular functions and relevant diseases of TAOKs, novel STE20 kinase family members. Curr. Pharmaceut. Des. *26*, 3122–3133. https://doi.org/10.2174/1381612826666200203115458.
38. de Anda, F.C., Rosario, A.L., Durak, O., Tran, T., Gräff, J., Meletis, K., Rei, D., Soda, T., Madabhushi, R., Ginty, D.D., et al. (2012). Autism spectrum disorder susceptibility gene TAOK2 affects basal dendrite formation in the neocortex. Nat. Neurosci. *15*, 1022–1031. https://doi.org/10.1038/nn.3141.
39. Yadav, S., Oses-Prieto, J.A., Peters, C.J., Zhou, J., Pleasure, S.J., Burlingame, A.L., Jan, L.Y., and Jan, Y.N. (2017). TAOK2 kinase mediates PSD95 stability and dendritic spine maturation through septin7 phosphorylation. Neuron *93*, 379–393. https://doi.org/10.1016/j.neuron.2016.12.006.
40. McNeer, J.L., Goussetis, D.J., Sassano, A., Dolniak, B., Kroczynska, B., Glaser, H., Altman, J.K., and Platanias, L.C. (2010). Arsenic trioxide-dependent activation of thousand-and-one amino acid kinase 2 and transforming growth factor-beta-activated kinase 1. Mol. Pharmacol. *77*, 828–835. https://doi.org/10.1124/mol.109.061507.
41. Wojtala, R.L., Tavares, I.A., Morton, P.E., Valderrama, F., Thomas, N.S.B., and Morris, J.D.H. (2011). Prostate-derived sterile 20-like kinases (PSKs/TAOKs) are activated in mitosis and contribute to mitotic cell rounding and spindle positioning. J. Biol. Chem. *286*, 30161–30170. https://doi.org/10.1074/jbc.M111.228320.
42. Chen, K., Lai, C., Su, Y., Bao, W.D., Yang, L.N., Xu, P.P., and Zhu, L.Q. (2022). cGAS-STING-mediated IFN-I response in host defense and neuroinflammatory diseases. Curr. Neuropharmacol. *20*, 362–371. https://doi.org/10.2174/1570159X19666210924110144.
43. Lee, J.D., and Woodruff, T.M. (2021). TDP-43 puts the STING in ALS. Trends Neurosci. *44*, 81–82. https://doi.org/10.1016/j.tins.2020.12.001.
44. Paul, B.D., Snyder, S.H., and Bohr, V.A. (2021). Signaling by cGAS-STING in neurodegeneration, neuroinflammation, and aging. Trends Neurosci. *44*, 83–96. https://doi.org/10.1016/j.tins.2020.10.008.
45. Wu, J., Li, X., Zhang, X., Wang, W., and You, X. (2022). What role of the cGAS-STING pathway plays in chronic pain? Front. Mol. Neurosci. *15*, 963206. https://doi.org/10.3389/fnmol.2022.963206.
46. Deng, M., Chen, S.R., and Pan, H.L. (2019). Presynaptic NMDA receptors control nociceptive transmission at the spinal cord level in neuropathic pain. Cell. Mol. Life Sci. *76*, 1889–1899. https://doi.org/10.1007/s00018-019-03047-y.
47. Chen, W., McRoberts, J.A., Ennes, H.S., and Marvizon, J.C. (2021). cAMP signaling through protein kinase A and Epac2 induces substance P release in the rat spinal cord. Neuropharmacology *189*, 108533. https://doi.org/10.1016/j.neuropharm.2021.108533.
48. Chapman, K.B., Groenen, P.S., Vissers, K.C., van Helmond, N., and Stanton-Hicks, M.D. (2021). The pathways and processes underlying spinal transmission of low back pain: observations from dorsal root ganglion stimulation treatment. Neuromodulation *24*, 610–621. https://doi.org/10.1111/ner.13150.
49. Comitato, A., and Bardoni, R. (2021). Presynaptic inhibition of pain and touch in the spinal cord: from receptors to circuits. Int. J. Mol. Sci. *22*, 414. https://doi.org/10.3390/ijms22010414.
50. Uta, D., Kato, G., Doi, A., Andoh, T., Kume, T., Yoshimura, M., and Koga, K. (2019). Animal models of chronic pain increase spontaneous glutamatergic transmission in adult rat spinal dorsal horn in vitro and in vivo. Biochem.

Biophys. Res. Commun. *512*, 352–359. https://doi.org/10.1016/j.bbrc.2019.03.051.

51. Ma, S.B., Xian, H., Wu, W.B., Ma, S.Y., Liu, Y.K., Liang, Y.T., Guo, H., Kang, J.J., Liu, Y.Y., Zhang, H., et al. (2020). CCL2 facilitates spinal synaptic transmission and pain via interaction with presynaptic CCR2 in spinal nociceptor terminals. Mol. Brain *13*, 161. https://doi.org/10.1186/s13041-020-00701-6.
52. Zhang, G.F., Chen, S.R., Jin, D., Huang, Y., Chen, H., and Pan, H.L. (2021). Alpha2delta-1 upregulation in primary sensory neurons promotes NMDA receptor-mediated glutamatergic input in resiniferatoxin-induced neuropathy. J. Neurosci. *41*, 5963–5978. https://doi.org/10.1523/JNEUROSCI.0303-21.2021.
53. Shi, G., Zhou, X., Wang, X., Zhang, X., Zhang, P., and Feng, S. (2020). Signatures of altered DNA methylation gene expression after central and peripheral nerve injury. J. Cell. Physiol. *235*, 5171–5181. https://doi.org/10.1002/jcp.29393.
54. Cheng, Y.C., Snavely, A., Barrett, L.B., Zhang, X., Herman, C., Frost, D.J., Riva, P., Tochitsky, I., Kawaguchi, R., Singh, B., et al. (2021). Topoisomerase I inhibition and peripheral nerve injury induce DNA breaks and ATF3-associated axon regeneration in sensory neurons. Cell Rep. *36*, 109666. https://doi.org/10.1016/j.celrep.2021.109666.
55. Wang, H., Huo, X., Han, C., Ning, J., Chen, H., Li, B., Liu, J., Ma, W., Li, Q., Yu, Y., and Shi, K. (2021). Ferroptosis is involved in the development of neuropathic pain and allodynia. Mol. Cell. Biochem. *476*, 3149–3161. https://doi.org/10.1007/s11010-021-04138-w.
56. Li, G.Z., Hu, Y.H., Lu, Y.N., Yang, Q.Y., Fu, D., Chen, F., and Li, Y.M. (2023). CaMKII and Ca(V)3.2 T-type calcium channel mediate Connexin-43-dependent inflammation by activating astrocytes in vincristine-induced neuropathic pain. Cell Biol. Toxicol. *39*, 679–702. https://doi.org/10.1007/s10565-021-09631-y.
57. Zimmermann, M. (1983). Ethical guidelines for investigations of experimental pain in conscious animals. Pain *16*, 109–110. https://doi.org/10.1016/0304-3959(83)90201-4.
58. Bennett, G.J., and Xie, Y.K. (1988). A peripheral mononeuropathy in rat that produces disorders of pain sensation like those seen in man. Pain *33*, 87–107. https://doi.org/10.1016/0304-3959(88)90209-6.
59. Lin, J.P., Chen, C.Q., Huang, L.E., Li, N.N., Yang, Y., Zhu, S.M., and Yao, Y.X. (2018). Dexmedetomidine attenuates neuropathic pain by inhibiting P2X7R expression and ERK phosphorylation in rats. Exp. Neurobiol. *27*, 267–276. https://doi.org/10.5607/en.2018.27.4.267.
60. Qiu, Y., Chen, W.Y., Wang, Z.Y., Liu, F., Wei, M., Ma, C., and Huang, Y.G. (2016). Simvastatin attenuates neuropathic pain by inhibiting the RhoA/LIMK/Cofilin pathway. Neurochem. Res. *41*, 2457–2469. https://doi.org/10.1007/s11064-016-1958-1.
61. Qin, J., Li, A., Huang, Y., Teng, R.H., Yang, Y., and Yao, Y.X. (2020). CXCR3 contributes to neuropathic pain via ERK activation in the anterior cingulate cortex. Biochem. Biophys. Res. Commun. *531*, 166–171. https://doi.org/10.1016/j.bbrc.2020.07.104.
62. Huang, L.E., Guo, S.H., Thitiseranee, L., Yang, Y., Zhou, Y.F., and Yao, Y.X. (2018). N-methyl D-aspartate receptor subtype 2B antagonist, Ro 25-6981, attenuates neuropathic pain by inhibiting postsynaptic density 95 expression. Sci. Rep. *8*, 7848. https://doi.org/10.1038/s41598-018-26209-7.
63. Li, H.L., Huang, Y., Zhou, Y.L., Teng, R.H., Zhou, S.Z., Lin, J.P., Yang, Y., Zhu, S.M., Xu, H., and Yao, Y.X. (2020). C-X-C motif chemokine 10 contributes to the development of neuropathic pain by increasing the permeability of the blood-spinal cord barrier. Front. Immunol. *11*, 477. https://doi.org/10.3389/fimmu.2020.00477.

STAR★METHODS

KEY RESOURCES TABLE

REAGENT or RESOURCE	SOURCE	IDENTIFIER
Antibodies		
Rabbit-*anti*-TAOK2	GeneTex	Cat# GTX111170; RRID: AB_10632858
Rabbit-*anti*-pTAOK2	GeneTex	Cat# GTX82581; RRID: AB_11165606
Rabbit-*anti*-cGAS	Cell Signaling Technology	Cat# 79978; RRID: AB_2905508
Rabbit-*anti*-STING	Cell Signaling Technology	Cat# 13647; RRID: AB_2732796
Rabbit-*anti*-STING	Proteintech	Cat# CL647-80165; RRID: AB_2920332
Mouse-*anti*-tubulin	Beyotime Biotechnology	Cat# AF2827; N/A
Mouse-*anti*-GAPDH	Proteintech	Cat# 60004-1-Ig; RRID: AB_2107436
Goat-*anti*-Iba1	Abcam	Cat# ab5076; RRID: AB_2224402
Mouse anti-GFAP	Cell Signaling Technology	Cat# 3670; RRID: AB_561049
Mouse-*anti*-NeuN	Abcam	Cat# ab104224; RRID: AB_10711040
Mouse-*anti*-CGRP	Abcam	Cat# ab81887; RRID: AB_1658411
Chemicals, peptides, and recombinant proteins		
FDbio-Femto ECL kit	FDbio Science Biotech Co.,Ltd	Cat# FD8030
BCA Protein Assay Kit	FDbio Science Biotech Co.,Ltd	Cat# FD2001
Polyethylenimine	Polyplus	Cat# 26032C1D
siRNA-TAOK2	Sangon Biotech Co. Ltd.	Cat# N/A
RU.521	Selleck	Cat# S6841
C-176	Selleck	Cat# S6575
Nocodazole	Selleck	Cat# S2775
Dimethyl sulfoxide	Sigma	Cat# D2650
AAV-shRNA-STING	Hanheng Biotechnology Co. Ltd.	Cat# N/A
Experimental models: Organisms/strains		
Rat: Sprague-Dawley		N/A
Software and algorithms		
GraphPad Prism V 8.0	GraphPad Software	https://www.graphpad.com/
Image Lab V 5.2	Bio-Rad	https://www.bio-rad.com/
Others		
ChemiDoc MP System	Bio-Rad	https://www.bio-rad.com/
Olympus FV3000	Olympus	https://www.olympus.com.cn/

RESOURCE AVAILABILITY

Lead contact

Further information and requests for resources and reagents should be directed to and will be fulfifilled by the lead contact, Dr. Yong-Xing Yao (yaoyongxing@zju.edu.cn).

Materials availability

This study did not generate new unique reagents.

Data and code availability

- All data reported in this paper will be shared by the lead contact on request.
- This paper does not report original code.
- Any additional information required to reanalyze the data reported in this paper is available from the lead contact on request.

EXPERIMENTAL MODEL AND SUBJECT DETAILS

Animals

Male Sprague–Dawley rats (around 8 weeks; weight, 220 ± 20 g) were provided by the Experimental Animal Center of the Zhejiang Academy of Medical Sciences. Rats were housed in a temperature-controlled environment (24 ± 2°C), followed by a 12-h light–dark cycle, and were randomly fed a standard diet and water. The rats were given one week to adapt to the new environment before the experiment and were randomly allocated to each group. All animal experiments complied with the ARRIVE guidelines, internationally accredited guidelines, and ethical regulations on animal research.[57] The study protocol was approved by the Research Ethics Committee of the First Affiliated Hospital of Zhejiang University. All efforts were made to minimize the number and suffering of animals.

METHODS DETAILS

CCI surgery

The rats were randomly allocated to the naive, sham, and CCI groups. The rats were anesthetized with isoflurane, as described in our previous studies and a study by Bennett and Xie.[58,59] A 1 cm incision was made, and the subsequent blunt dissection of muscles was performed in the middle thigh to expose the left sciatic nerve. In the CCI group, following isolation, the sciatic nerve was ligated using three strands of 4-0 chromic gut sutures (Pudong Jinghuan Co. Ltd., Shanghai, China) 1 mm apart. Thereafter, the muscles and skin were closed with 4-0 sutures layer by layer. In the sham group, the sciatic nerve was exposed yet not ligated. In the naive group, the rats did not undergo any surgical procedures. The rats were administered a subcutaneous injection of 80,000 U penicillin (North China Pharmaceutical Co. Ltd., Hebei, China) to prevent infection.

Intrathecal catheterization and drug administration

According to a previously described protocol,[60] a PE-10 catheter (length, 12 cm) was implanted intrathecally under anesthesia with isoflurane. Briefly, a 1 cm longitudinal incision was made above the L5–6 vertebrae. The subcutaneous fascia was removed with ophthalmic scissors to fully expose the spine, and the erector spinae was bluntly separated on the right side of the spine using forceps. A 23-gauge needle was used to puncture the ligamentum flavum in the intervertebral space. The catheter was pushed through the intervertebral space toward the head until the sudden movement of the tail or hindlimb was observed and fixed with 4-0 sutures. The tip of the catheter was fixed at the neck area of the rat through a subcutaneous channel. Catheter localization was verified by intrathecal injection of 2% 15 μL lidocaine, and catheterization was successful if there was transient weakness in both hindlimbs. Rats were allowed to recover for 5 days after catheterization prior to further experiments. Nocodazole, RU.521, and C-176 were purchased from Selleck (Houston, TX, USA) and dissolved in DMSO (10%) to 20 μg/10 μL. PEI and TAOK2-siRNA were obtained from Sangon Biotech Co. Ltd. (Shanghai, China). AAV-shRNA-STING (1×10^{13} vg/mL) was purchased from Hanheng Biotechnology Co. Ltd. (Shanghai, China). Nocodazole (20 μg a day) was injected for two consecutive days. The TAOK2-siRNA (10 μg a day) was injected on days 7 and 8 after CCI. RU.521 and C-176 (20 μg a day) were injected on days 7 and 8 after CCI. AAV-shRNA-STING (10 μL) was injected 3 weeks before the CCI.

Behavioral tests

All rats were acclimated to the climate in a plastic box (12 cm × 15 cm × 22 cm) on an elevated wire mesh for 3 consecutive days (30 min a day) before experiments, and the behavioral experimenter was blinded to the experimental protocol.

The MWT was assessed using von Frey filaments, according to our previous report.[59] Briefly, the tip of filaments was placed on the plantar surface of the left hind paw with an increased stiffness of 0.4 g–26 g until a quick withdrawal or licking of the paw was observed, and the magnitude of the filaments was recorded as the MWT. The test was repeated three times with an interval of 5 min, and the average value was considered as the final MWT.

As described in our previous study,[61] the ATS was measured using the same apparatus as the MWT test to denote cold allodynia. Briefly, 100 μL of acetone was sprayed onto the left plantar surface, and responses were observed for 20 s after application. The results were scored on a 4-point scale: 0, no response or startle response without paw withdrawal; 1, brief withdrawal of the paw; 2, prolonged withdrawal; and 3, prolonged and repetitive withdrawal along with flinching or licking of the hind paw. The testing was repeated three times at an interval of 5 min, and the average value was considered as the final ATS.

Western blot analysis

The Western blot protocols were performed according to our previous studies.[62] After deep anesthesia with pentobarbital sodium, rats were decapitated, and lumbar enlargement of the spinal cord was quickly harvested and divided into four parts. The dorsal horns were selected and homogenized on ice using a lysis buffer containing protease and phosphatase inhibitors. The tissue homogenates were separated by 10% SDS-PAGE and subsequently transferred to 0.45-μm PVDF membranes. The membranes were blocked with 5% skimmed milk at 24°C for 1 h. Thereafter, membranes were incubated with the following primary antibodies for 24 h at 4°C: rabbit-*anti*-TAOK2 (1:500; GeneTex, TX, USA), rabbit-*anti*-pTAOK2 (1:1000, GeneTex), rabbit-*anti*-cGAS (1:1000, Cell Signaling Technology, Mass, USA), rabbit-*anti*-STING (1:500, Cell Signaling Technology), mouse-*anti*-tubulin (1:2000, Beyotime Biotechnology, Shanghai, China), and mouse-*anti*-GAPDH (1:10,000, Proteintech, IL, USA). After washing the primary antibody in TBST, the membrane was incubated with HRP-conjugated secondary antibody for 2 h at 24°C. The ChemiDoc MP System (Bio-Rad, Hercules, CA, USA) was used to detect the immune complex bands.

Immunofluorescence assay

According to our previous report,[63] after being deeply anesthetized with pentobarbital sodium, rats were transcardially perfused with 150 mL of 1× PBS (4°C) followed by 150 mL of 4% paraformaldehyde (4°C). Lumbar enlargement of the spinal cord was collected, postfixed in 4% paraformaldehyde for 48 h at 4°C, and subsequently dehydrated with 30% sucrose for 3 days at 4°C. Subsequently, the spinal cord was cut transversely into slices with a thickness of 30 μm. The sections were permeabilized with 0.3% Triton X-100 for 10 min and blocked with 10% sheep or donkey serum for 2 h at 24°C. Sections were incubated with the following primary antibodies for 48 h at 4°C: goat-*anti*-Iba1 (1:200, Abcam, Cambridge, UK), mouse anti-GFAP (1:500, Cell Signaling Technology), mouse-*anti*-NeuN (1:500, Abcam), rabbit-*anti*-pTAOK2 (1:100, GeneTex), rabbit-*anti*-cGAS (1:100, Cell Signaling Technology), and rabbit-*anti*-STING (1:100, Cell Signaling Technology). After washing with 1× PBS, the sections were incubated with fluorescent secondary antibodies in the dark for 2 h at 24°C. Finally, the sections were examined under a fluorescence microscope (FV3000; Olympus, Japan).

QUANTIFICATION AND STATISTICAL ANALYSIS

All data are expressed as the mean ± SEM, and statistical analyses were performed using Prism 8.0 software (GraphPad, San Diego, CA, USA). Western blot data and behavioral tests at single time points were analyzed using one-way analysis of variance (ANOVA) followed by LSD. Behavioral tests across different time points were analyzed using two-way ANOVA followed by Tukey's multiple comparisons test. Statistical significance was set at $p < 0.05$.